Supplementary Information

Combined Experimental and DFT Studies of Amino acid Adsorption on Biomimetic Apatite: Application to Serine

Youness Hajji, Christophe Drouet, Stéphanie Sarda * and Corinne Lacaze-Dufaure

Univ. Toulouse, CNRS, Toulouse INP, CIRIMAT, Toulouse, France

*Corresponding author. E-mail: stephanie.sarda@iut-tlse3.fr

I. *Analysis of the synthetic biomimetic apatite*

Table S1: Frequencies obtained from the spectral decomposition of the $\nu_4(PO_4)$ domain for biomimetic apatite and peaks area. In this table, the notation (*a*) refers to bands assigned to apatitic environments, while (*na*) refers to bands associated with non-apatitic environments related to the presence of the hydrated ionic layer.

Assignment	Biomimetic apatite (cm^{-1})	Peaks area
$\nu_2(PO_4)$ (*a*)	469	0.04310
$\nu_4(HPO_4)$ (*na*)	534	1.13652
$\nu_4(HPO_4)$ (*a*)	550	0.46871
$\nu_4(PO_4)$ (*a*)	561	0.88433
$\nu_4(PO_4)$ (*a*)	575	1.12776
$\nu_4(PO_4)$ (*a*)	603	1.06622
$\nu_4(PO_4)$ (*na*)	617	0.04496
$\nu_{lib}(OH)$ (*a*)	632	0.84062
$\nu_{lib}(H_2O)$	670	0.30868

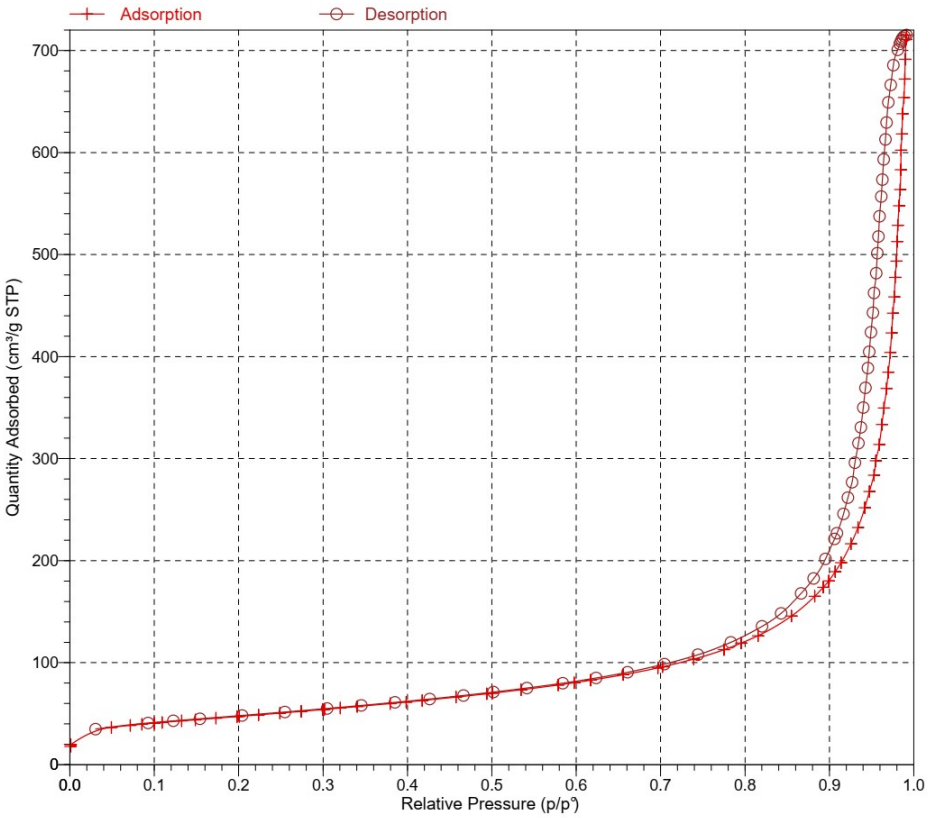

Figure S1: BET isotherms for the specific surface measurement of the synthesized biomimetic apatite. The specific surface area of the biomimetic apatite powders was evaluated by nitrogen adsorption using the BET method, on an ASAP 2020 equipment (Micrometrics). Before measurement, the powder was outgassed at 80°C for a period of 12 hours, with all measurements performed in triplicate to ensure reproducibility and accuracy.

II. *Liquid water and biomimetic apatite/water model*

In this study, *ab initio* molecular dynamics (AIMD) simulations were used to model bulk liquid water, the biomimetic apatite/water interface, and to generate initial configurations for serine adsorption. All simulations were performed in the canonical (NVT) at 300 K using the VASP code. Throughout the AIMD simulations, electronic structure calculations were performed using a plane-wave cutoff energy of 400 eV, an electronic convergence threshold of 10^{-6} eV, and a (1 × 1 × 1) k-point mesh centered at the Γ point.

To model bulk liquid water, a 30 ps AIMD simulation was conducted. For the biomimetic apatite/water interface, a 10 ps simulation was performed to allow sufficient equilibration of the water layer at the interface with the atoms of the biomimetic apatite model kept fixed,

while only the water molecules allowed to move. The temperature was maintained at 300 K using a Nosé–Hoover thermostat [1–3], with a time step of 1 fs.

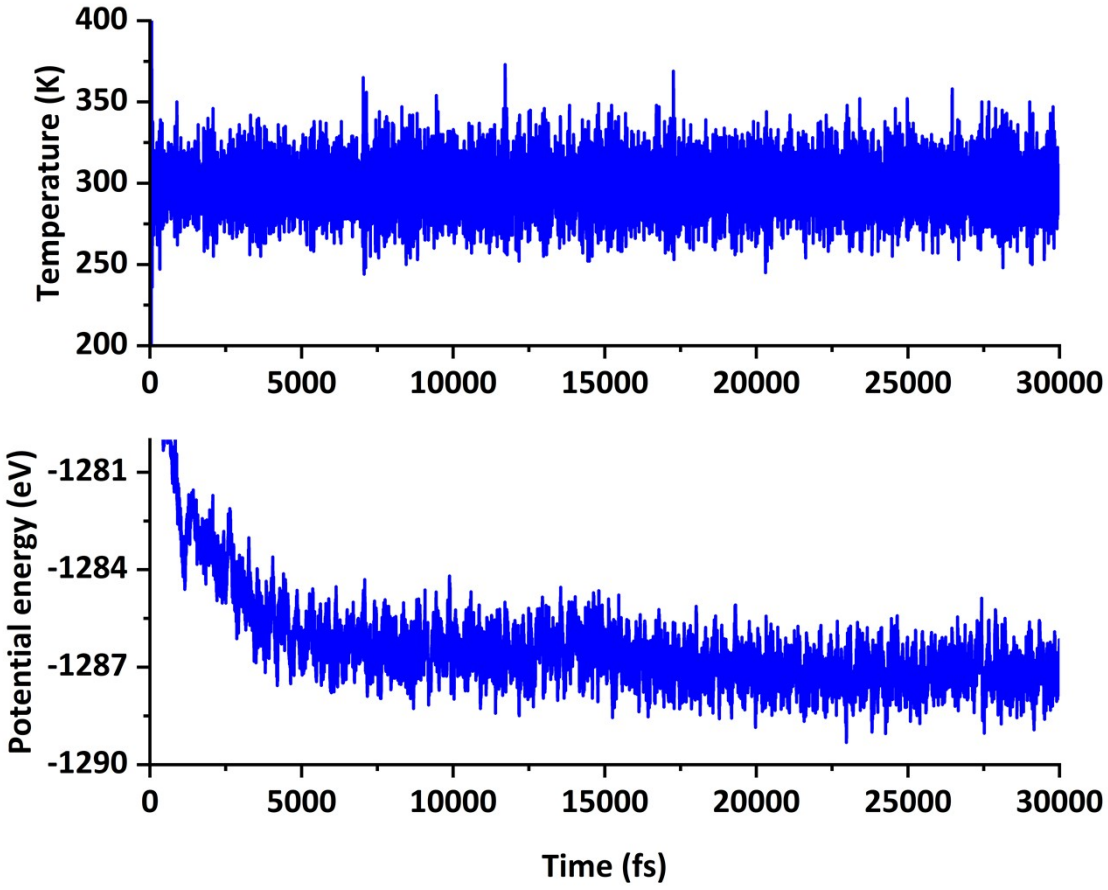

Figure S2: Calculated values of the temperature and the potential energy of the bulk liquid water along the AIMD trajectory (30 ps).

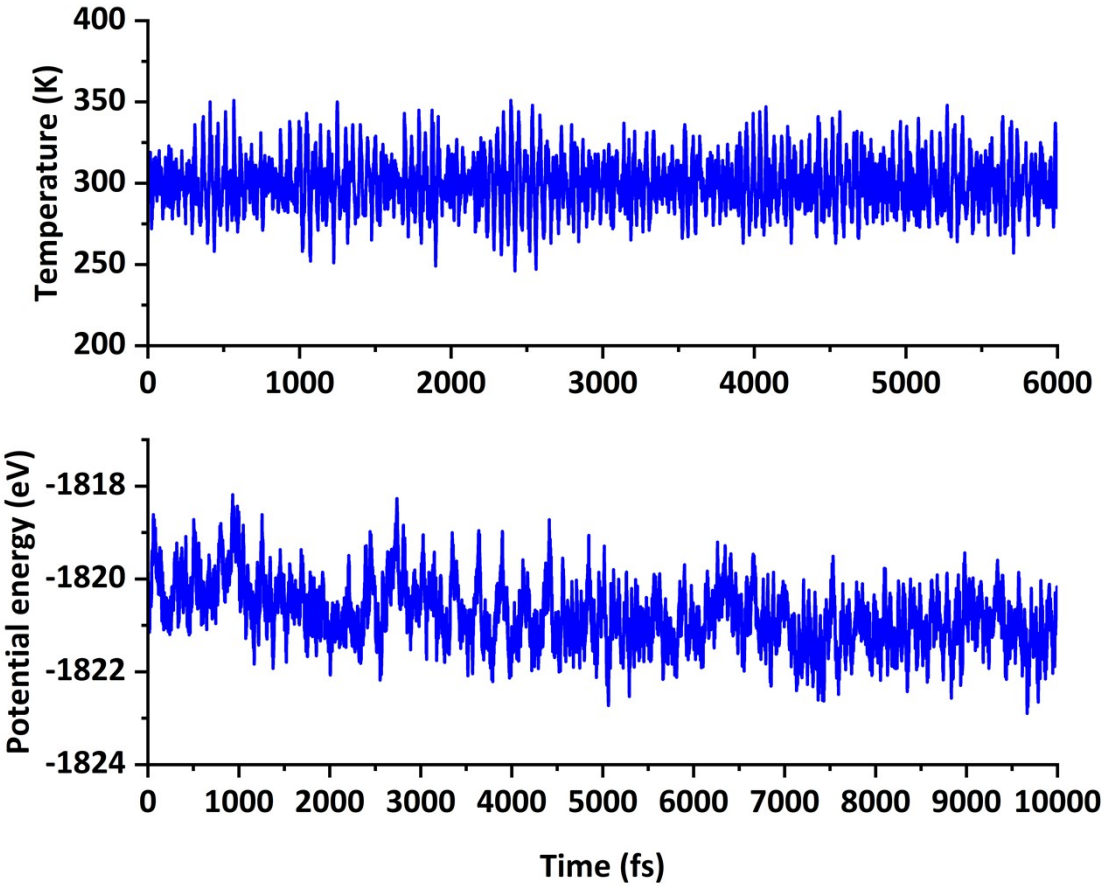

Figure S3: Calculated values of the temperature and the potential energy of the liquid water/biomimetic apatite interface along the AIMD trajectory (10 ps).

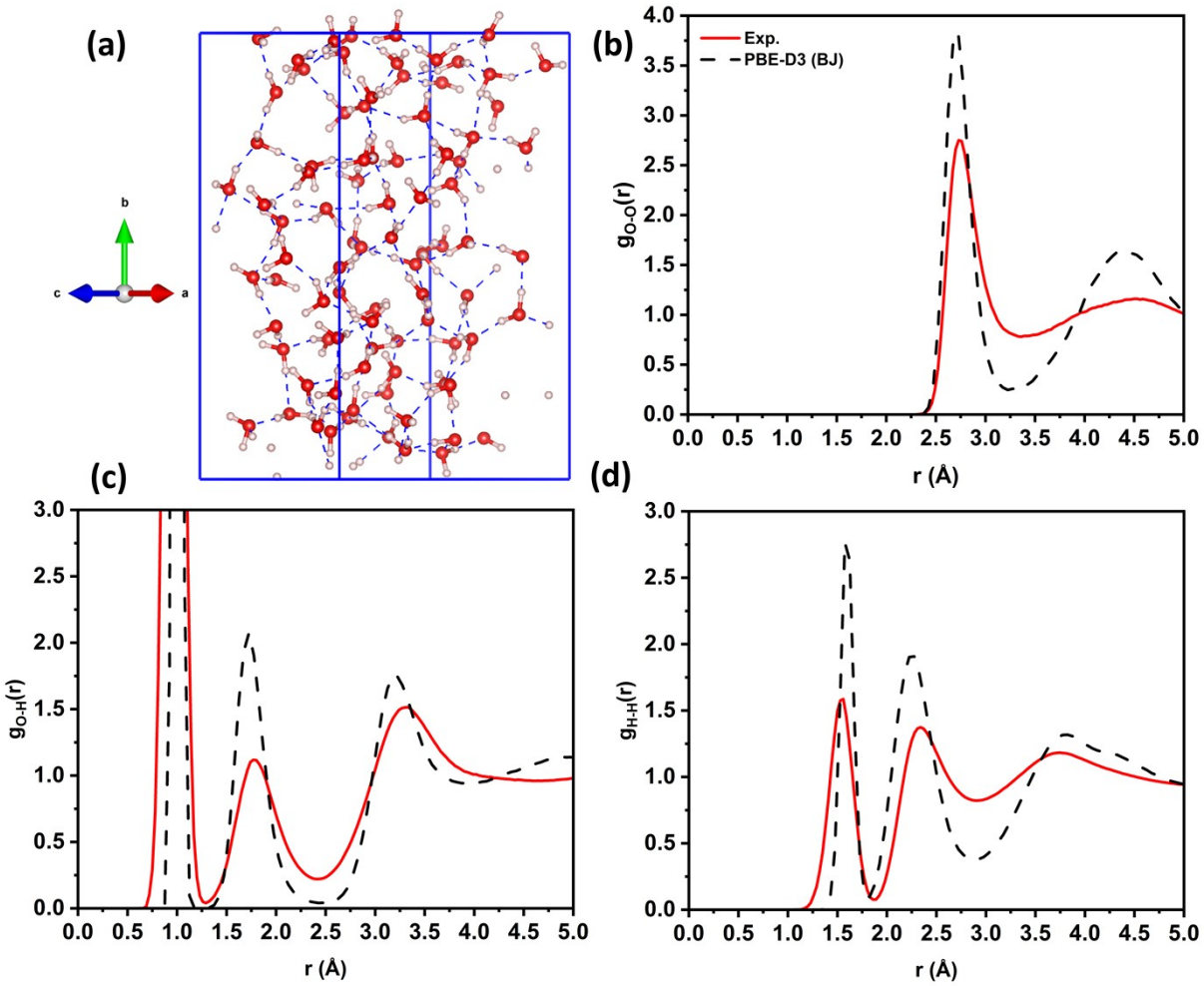

Figure S4: (a) Orthorhombic simulation cell containing 87 water molecules with a density equivalent to that of liquid water at 298 K (1 g/cm³); (b–d) Oxygen-oxygen, oxygen-hydrogen and hydrogen-hydrogen radial distribution functions of liquid water simulations, compared to neutron scattering experimental data.

For bulk liquid water, the simulation cell consisted of 87 water molecules, corresponding to the experimental density of liquid water at 298 K (~1 g/cm³). The dimensions of the orthorhombic simulation cell in the *a* and *c* directions were chosen to match those of the biomimetic apatite slab model used in subsequent simulations, ensuring structural consistency across all systems (see Figure S4(a)).

After equilibration of the water system, structural data was extracted by computing radial distribution functions (RDFs) for O–O, O–H, and H–H atomic pairs. These RDFs provide insight into the short-range order and hydrogen bonding network in liquid water. The computed RDFs (Figures S4(b–d)) were compared with experimental data obtained from neutron scattering measurements [4].

The O–O RDF (see Figure S4(b)) displays a first peak centered at approximately 2.73 Å, in close agreement with the experimental peak at ~2.75 Å. Similarly, the positions of the first peaks in the O–H and H–H RDFs (Figures S4(c) and (d)) are consistent with neutron diffraction data, confirming that the local structuration of water molecules is well captured by our model. The first peaks in the RDFs are slightly higher than those observed experimentally. This overstructuration has been thoroughly documented as an artifact of density functional theory (DFT)-based simulations of liquid water, especially when using GGA functionals [5–7].

Overall, the structural agreement between simulation and experiment supports the validity of the model for further investigation. The equilibrated water configuration obtained from this simulation was used as the starting point for constructing the hydrated biomimetic apatite surface model.

III. *Serine adsorption*

To generate initial adsorption configurations for serine, all computational parameters were kept consistent with those described above, except for the temperature, which was raised to 500 K. This increase was intended to enhance the mobility of the serine molecule and facilitate the sampling of a wide range of adsorption conformations. Three distinct initial geometries were built and individually simulated for 6 ps using AIMD. Representative snapshots were then selected from the resulting trajectories based on configurational diversity. Only the most distinct configurations were subsequently subjected to static DFT optimization to determine their relative energies and interaction characteristics with the biomimetic apatite surface.

The final geometries selected from the AIMD simulations were further optimized using more stringent parameters: a cutoff energy of 700 eV, an electronic convergence criterion of 10^{-6} eV, and a force convergence threshold of 10^{-2} eV/Å. These optimized structures were then used for analyzing the adsorption behavior of serine on the hydrated biomimetic apatite surface.

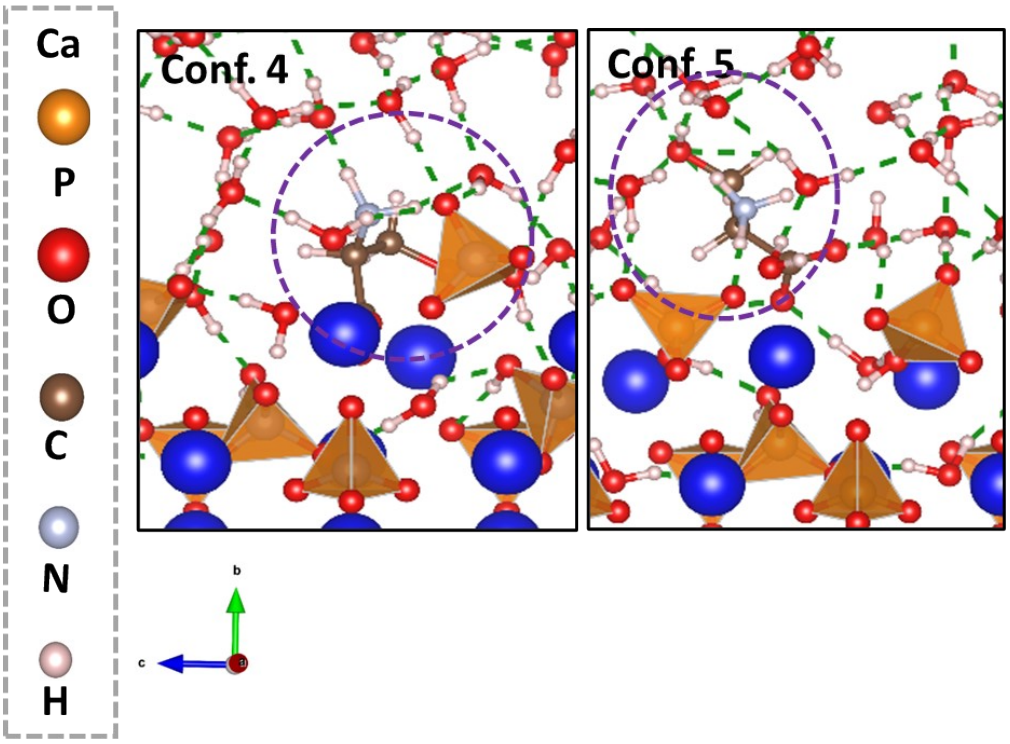

Figure S5: Additional adsorption geometries of zwitterionic serine on the biomimetic apatite surface in aqueous conditions. Each conformation highlights distinct interaction patterns between the molecule, the mineral surface, and the surrounding interfacial water. These models are provided in addition to the three representative configurations shown in Figure 6.

Table S2: Computed relative energies (ΔE_{rel}, in eV, compared to Conf. 1), and adsorption energies (E_{ads}, in eV) for five serine adsorption configurations on the biomimetic apatite surface in the presence of an explicit solvent. Conf. 4 and Conf. 5 are additional serine adsorption configurations not presented main manuscript.

E_{ads}^{elec} and E_{ads}^{disp} refer to the DFT and dispersion components of the adsorption energy, repectively. ΔQ_{ser} is the charge variation on the serine molecule upon adsorption.

Configurations	ΔE_{rel} **(eV)**	E_{ads} **(eV)**	E_{ads}^{elec} (eV)	E_{ads}^{disp} (eV)	ΔQ_{ser} (e)
Conf. 1	0.000	-0.918	-0.876	-0.042	0.00

Conf. 2	0.175	-0.744	-0.737	-0.007	0.03
Conf. 3	0.517	-0.401	-0.535	0.134	-0.01
Conf. 4	0.663	-0.255	-0.363	0.108	-0.01
Conf. 5	0.875	-0.044	-0.277	0.234	0.04

Conf. 4

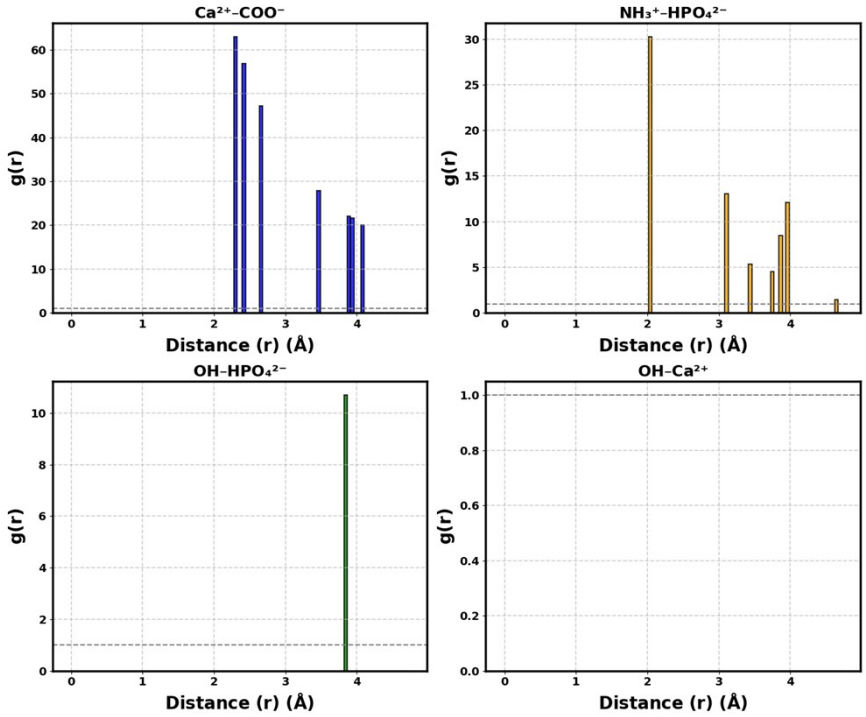

Conf. 5

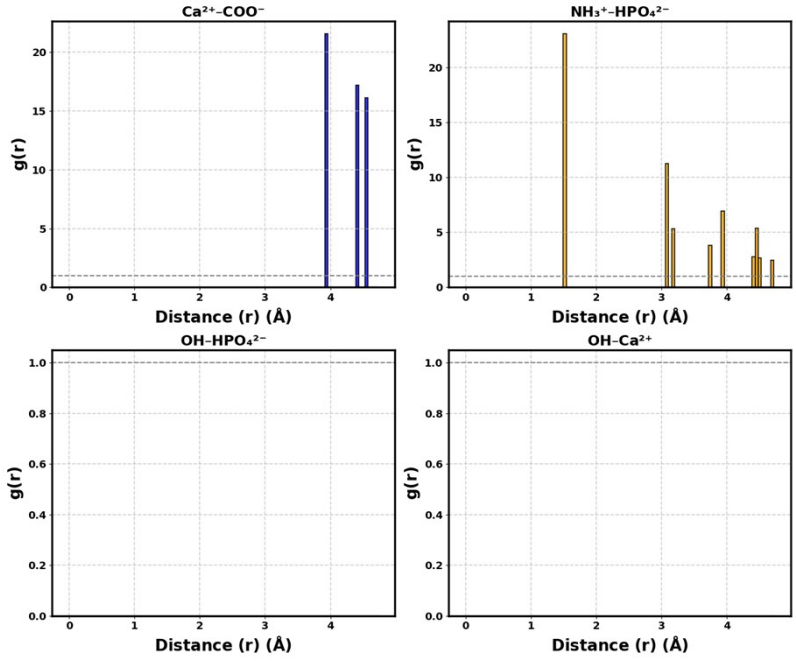

Figure S6: RDFs for favored conformations of the serine adsorbed on the biomimetic apatite model, in the presence of water molecules ($^{\Delta E_{rel}}$ ≥ 0.52 eV see Table S2).

Additional references:

1 S. Nosé, *The Journal of chemical physics*, 1984, **81**, 511–519.

2 N. Shuichi, *Progress of Theoretical Physics Supplement*, 1991, **103**, 1–46.

3 W. G. Hoover, *Phys. Rev. A*, 1985, **31**, 1695–1697.

4 A. K. Soper, *ISRN Physical Chemistry*, 2013, **2013**, 1–67.

5 M. V. Fernández-Serra and E. Artacho, *The Journal of chemical physics*, 2004, **121**, 11136–11144.

6 J. VandeVondele, F. Mohamed, M. Krack, J. Hutter, M. Sprik and M. Parrinello, *J Chem Phys*, 2005, **122**, 14515.

7 L.-M. Liu, M. Krack and A. Michaelides, *J Chem Phys*, 2009, **130**, 234702.